Bismuth Qubits in Silicon: The Role of EPR Cancellation Resonances

M. H. Mohammady,[1] G. W. Morley,[1,2] and T. S. Monteiro[1]

[1]*Department of Physics and Astronomy, University College London, Gower Street, London WC1E 6BT, United Kingdom*

[2]*London Centre for Nanotechnology, University College London, Gordon Street, London WC1H 0AH, United Kingdom*

(Received 29 April 2010; published 6 August 2010)

We investigate electron paramagnetic resonance spectra of bismuth-doped silicon, at intermediate magnetic fields $B \simeq 0.1$–0.6 T, theoretically and experimentally (with 9.7 GHz X-band spectra). We identify a previously unexplored regime of "cancellation resonances," where a component of the hyperfine coupling is resonant with the external field. We show that this regime has experimentally accessible consequences for quantum information applications, such as reduction of decoherence, fast manipulation of the coupled electron-nuclear qubits, and spectral line narrowing.

DOI: 10.1103/PhysRevLett.105.067602 PACS numbers: 76.30.−v, 03.67.Lx, 71.55.Cn, 76.90.+d

Following Kane's suggestion [1] for using phosphorus-doped silicon as a source of qubits for quantum computing, there has been intense interest in such systems [2]. The phosphorus system (^{31}P) is appealing in its simplicity: It represents a simple electron-spin qubit $S = \frac{1}{2}$ coupled to a nuclear-spin qubit $I = \frac{1}{2}$ via an isotropic hyperfine interaction $A\mathbf{I}.\mathbf{S}$ of moderate strength ($\frac{A}{2\pi} = 117.5$ MHz). However, recent developments [3–5] point to Si:Bi (bismuth-doped silicon) as a very promising new alternative. Two recent studies measured spin-dephasing times of over 1 ms at 10 K, which is longer than comparable (non-isotopically purified) materials, including Si:P [3,4]. Another group implemented a scheme for rapid (on a time scale of $\sim$100 μs) and efficient (of order 90%) hyperpolarization of Si:Bi into a single spin state [5].

Bismuth has an atypically large hyperfine constant $\frac{A}{2\pi} = 1.4754$ GHz and nuclear spin $I = \frac{9}{2}$. This makes its EPR spectra somewhat more complex than for phosphorus, and there is strong mixing of the eigenstates for external field $B \lesssim 0.6$ T. Mixing of Si:P states was studied experimentally in Ref. [6], by means of electrically detected magnetic resonance, but at much lower fields $B \lesssim 0.02$ T. Residual mixing in Si:Bi for $B = 2$–6 T, where the eigenstates are $\gtrsim$99.9% pure uncoupled eigenstates of both $\hat{I}_z$ and $\hat{S}_z$, was also proposed as important for the hyperpolarization mechanism of illuminated Si:Bi [5]. In Ref. [4] it was found that even a $\sim$30% reduction in the effective paramagnetic ratio $\frac{df}{dB}$ (where f is the transition frequency) leads to a detectable reduction in decoherence rates.

Below, we present an analysis of EPR spectra for Si:Bi, testing this against experimental spectra. We identify the points for which $\frac{df}{dB} = 0$, explaining them in a unified manner in terms of a series of EPR "cancellation resonances"; some are associated with avoided level crossings while others, such as a maximum shown in ENDOR [7] spectra at $B \approx 0.37$ T in Ref. [4], are of a quite different origin. These cancellation resonances represent, to the best of our knowledge, an unexplored regime in EPR spectroscopy, arising in systems with exceptionally high A and I. They are somewhat reminiscent of the so-called "exact cancellation" regime, widely used in ESEEM spectroscopy [7,8] but differ in essential ways: For instance, they affect both electronic and nuclear frequencies rather than only nuclear frequencies. They have important implications for the use of Si:Bi as a coupled electron-nuclear-qubit pair: We show that all potential spin operations may be carried out with fast EPR pulses (on nanosecond time scales) where, in contrast, most operations for Si:P require slower NMR pulses (on microsecond time scales). A striking spectral signature is reduced sensitivity to certain types of ensemble averaging, giving an analog to the ultranarrow lines well known in exact cancellation, as well as the reduction of decoherence. Further details are found in Ref. [9].

We model the Si:Bi spin system approximately by a Hamiltonian including an isotropic hyperfine coupling term:

$$\hat{H} = \omega_0 \hat{S}_z - \omega_0 \delta \hat{I}_z + A\hat{\mathbf{S}}.\hat{\mathbf{I}}, \tag{1}$$

where ω_0 represents the frequency of the magnetic field and $\delta = \omega_I/\omega_0 = 2.488 \times 10^{-4}$ represents the ratio of the nuclear to electronic Zeeman frequencies. For $I = \frac{9}{2}$, $S = \frac{1}{2}$ there are 20 eigenstates which can be superpositions of high-field eigenstates $|m_s, m_I\rangle$; but since $[\hat{H}, \hat{S}_z + \hat{I}_z] = 0$, the $|m_s, m_I\rangle$ basis is at most mixed into a doublet $|m_s = \pm\frac{1}{2}, m_I = m \mp \frac{1}{2}\rangle$ with constant $m = m_s + m_I$. One can thus write the Hamiltonian for each m subdoublet as a two-dimensional matrix H_m (where $H_m = \frac{A}{2}\tilde{h}_m$):

$$\tilde{h}_m = [m + \tilde{\omega}_0(1 + \delta)]\hat{\sigma}_z + (25 - m^2)^{1/2}\hat{\sigma}_x - (\tfrac{1}{2} + 2m\delta\tilde{\omega}_0)\mathbf{I} \tag{2}$$

and where $\tilde{\omega}_0 = \frac{\omega_0}{A}$ is the rescaled field, $\hat{\sigma}_z$ and $\hat{\sigma}_x$ represent Pauli matrices in the two-state basis $|m_s, m_I\rangle = |\pm\frac{1}{2}, m \mp \frac{1}{2}\rangle$, and $\mathbf{I}$ is the identity operator. It becomes clear that whenever $m = -\tilde{\omega}_0(1 + \delta) \simeq -\tilde{\omega}_0$, the quantum states become eigenstates of $\hat{\sigma}_x$; thus the eigenstates $|\pm, m\rangle$ assume Bell-like form: $|\pm, m\rangle = (1/\sqrt{2})[|-\frac{1}{2}\rangle|m+\frac{1}{2}\rangle \pm |+\frac{1}{2}\rangle|m-\frac{1}{2}\rangle]$. In contrast, exact cancellation results in a simple superposition of the nuclear states (which also allows other types of manipulations [10]). Since $\omega_0 \geq 0$, only states with $-5 \leq m \leq 0$ can yield resonances where the $\hat{\sigma}_z$ terms are eliminated. They occur at $\omega_0 \simeq 0, A, \ldots, 4A, 5A$, corresponding to applied field $B = 0, 0.053, \ldots, 0.21, 0.26$ T. Below, we show that all $\frac{df}{dB} = 0$ points which are minima occur midway between these resonances. But the $\frac{df}{dB} = 0$ maximum at the $\omega_0 = 7A \equiv 0.37$ T resonance, and seen in experiments [4], is shown to be of a different type.

It is standard practice to represent two-state quantum systems by using vectors on the Bloch sphere [8]. We define a parameter $R_m^2 = [m + \tilde{\omega}_0(1+\delta)]^2 + 25 - m^2$, where R_m represents the vector sum magnitude of spin x and z components. Denoting θ as the inclination to the z axis, $\cos\theta_m = [m + \tilde{\omega}_0(1+\delta)]/R_m$ and $\sin\theta_m = (25 - m^2)^{1/2}/R_m$; then Eq. (2) can also be written as

$$\tilde{h}_m = R_m \cos\theta_m \hat{\sigma}_z + R_m \sin\theta_m \hat{\sigma}_x - \tfrac{1}{2}(1 + 4\tilde{\omega}_0 m\delta)\mathbf{I}. \quad (3)$$

Straightforward diagonalization gives the pair of eigenstates, for each m, at arbitrary magnetic fields ω_0:

$$|\pm, m\rangle = a_m^\pm|\pm\tfrac{1}{2}, m \mp \tfrac{1}{2}\rangle + b_m^\pm|\mp\tfrac{1}{2}, m \pm \tfrac{1}{2}\rangle, \quad (4)$$

where

$$a_m^\pm = \frac{1}{\sqrt{2}}(1+\cos\theta_m)^{1/2}, \quad b_m^\pm = \pm\frac{1}{\sqrt{2}}\frac{\sin\theta_m}{(1+\cos\theta_m)^{1/2}}, \quad (5)$$

and the corresponding eigenenergies:

$$E_m^\pm(\omega_0) = \frac{A}{2}\left[-\frac{1}{2}(1 + 4\tilde{\omega}_0 m\delta) \pm R_m\right]. \quad (6)$$

In Fig. 1, the simple (but exact) Eq. (6) reproduces the spin spectra investigated in, e.g., Refs. [3,5]. Equations (5) are valid for all states except the unmixed $m = \pm 5$ states ($|10\rangle$ and $|20\rangle$). For $|m| = 5$, there is no $\hat{\sigma}_x$ coupling: These two states are unmixed for all magnetic fields; thus, $a_{\pm 5} = 1$ and $b_{\pm 5} = 0$ and Eq. (6) simplifies drastically to give $E_{m=\pm 5} = \pm\frac{1}{2}\omega_0 \mp \frac{9}{2}\omega_0\delta + \frac{9A}{4}$.

For the doublets, the $a_m^\pm$ are the dominant coefficients at high field. Then, the $B \to \infty$ limit corresponds to angle $\theta_m = 0$, so $a_m^\pm \to 1$ and $b_m^\pm \to 0$ and the states become uncoupled. The $|m| \leq 4$ cancellation resonances correspond to $\theta_m = \pi/2$ so $a_m^\pm = 1/\sqrt{2}$, while $b_m^\pm = \pm(1/\sqrt{2})$. The EPR emission transitions $|+, m\rangle \to |-, m-1\rangle$ are dipole allowed at all fields. Since the matrix elements $|\langle m_s = \frac{1}{2}|S_x|m_s' = -\frac{1}{2}\rangle|^2 = 1/2$ for all transitions, relative intensities $I_{m\to m-1}^{+\to -} = |a_m^+|^2|a_{m-1}^-|^2$ are [9]

$$I_{m\to m-1}^{+\to -} = \tfrac{1}{4}(1+\cos\theta_m)(1+\cos\theta_{m-1}). \quad (7)$$

If mixing is significant, $|+, m\rangle \to |+, m-1\rangle$ transitions (of intensity I_m^+) and $|-, m-1\rangle \to |-, m\rangle$ transitions (of intensity I_m^-), EPR-forbidden at high field, become strong, with relative intensities:

$$I_m^\pm = \tfrac{1}{4}(1 \pm \cos\theta_m)(1 \mp \cos\theta_{m-1}). \quad (8)$$

Forbidden lines disappear at high fields; as $\omega_0 \to \infty$, one can see from Eq. (5) that $I_{\pm, m\to m-1} \sim \frac{1}{\omega_0^2} \to 0$ since $|b_m^-|^2 \propto \frac{1}{\omega_0^2}$ at high fields. Equations (6)–(8) are exact and so are in complete agreement with numerical diagonalization of the full Hamiltonian.

In Fig. 2(a), we test the equations against experimental spectra at $\lesssim 0.6$ T and microwave frequency 9.67849 GHz. The long spin relaxation times at low temperatures means that the EPR spectra are easily saturated, complicating the analysis of the line intensities. We therefore used a temperature of 42 K so as to measure unsaturated resonances. The shorter relaxation times at these elevated temperatures may be due to the presence of significant numbers of conduction electrons that are no longer bound to Si:Bi donors. We measure a very broad microwave absorption centered on zero magnetic field [subtracted from Fig. 2(a)] which we attribute to these conduction electrons. The comparison with experiment shows excellent agreement with the positions of the resonances, which are far from equally spaced in the low-field regime. Experimental lines are found to be Gaussians of width ≈ 0.42 mT; this was attributed in Ref. [3] to the effects of ^{29}Si in this sample;

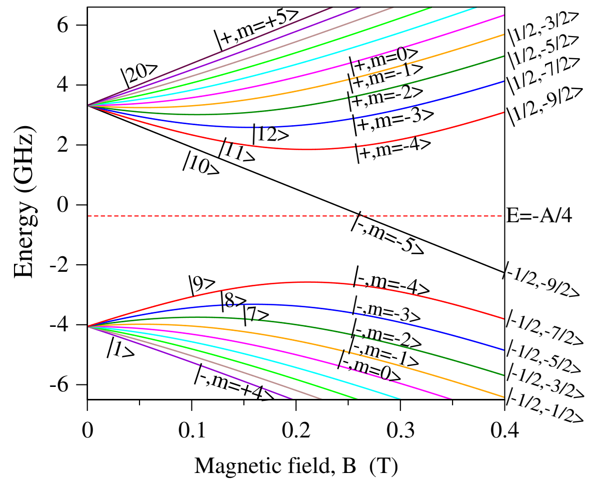

FIG. 1 (color online). The 20 spin energy levels of Si:Bi may be labeled in alternative ways: (i) in order of increasing energy $|1\rangle, |2\rangle, \ldots, |20\rangle$; (ii) by using the adiabatic basis $|\pm, m\rangle$ of doublets—levels belonging to the same doublet are shown in the same color (online); (iii) by their asymptotic, high-field form $|m_s, m_I\rangle$. States $|10\rangle$ and $|20\rangle$ are not mixed. State $|10\rangle$ is of special significance since it (rather than the ground state) is a favorable state to initialize the system in (experimental hyperpolarization studies [5] concentrate the system in this state). Thus, in our coupled 2-qubit scheme, state $|10\rangle$ corresponds to our $(0)_e(0)_n$ state; in the same scheme, states $|9\rangle \equiv (0)_e(1)_n$ and $|11\rangle \equiv (1)_e(0)_n$ are related to $|10\rangle$ by a single qubit flip (of either the electron or nuclear qubits, respectively), while for $|12\rangle \equiv (1)_e(1)_n$ both qubits are flipped.

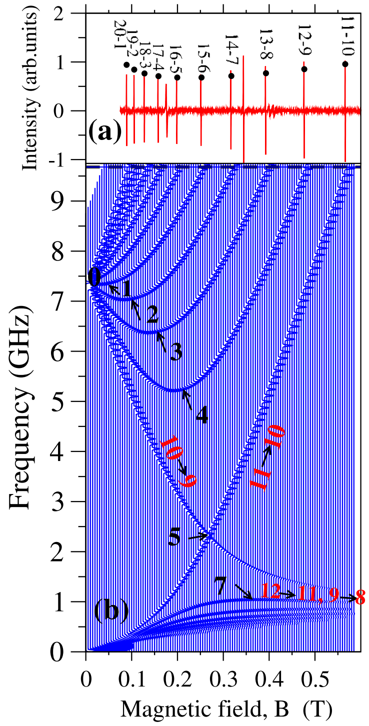

FIG. 2 (color online). (a) Comparison between theory [Eqs. (6) and (7)] (black dots) and experimental continuous wave EPR signal (red online) at 9.7 GHz. Resonances without black dots above them are not due to Si:Bi; the large sharp resonance at 0.35 T is due to silicon dangling bonds, while the remainder are due to defects in the sapphire ring used as a dielectric microwave resonator. The variation in relative intensities is mainly due to the mixing of states as in Eq. (4). The variability is not too high, but the calculated intensities are consistent with experiment and there is excellent agreement for the line positions. (b) Calculated EPR spectra (convolved with the 0.42 mT measured linewidth); they are seen to line up with the experimental spectra at $f = \frac{\omega}{2\pi} = 9.7$ GHz. The field values corresponding to $\tilde{\omega}_0 = 0, 1, 2, 3, 4\ldots$ and cancellation resonances are indicated by arrows. The $\tilde{\omega}_0 = 7$ maximum of $\frac{df}{dB}$ indicated by the integer 7 corresponds to that shown in the $\lesssim 2$ GHz ENDOR spectra of Ref. [4].

samples with enriched ^{28}Si are expected to give much narrower linewidths.

For Fig. 2(b), we generated the spectra, convolved with 0.42 mT Gaussians to obtain the EPR spectra of all lines (both allowed and forbidden) at all frequencies below 10 GHz. We indicate the main dipole allowed lines as well as the approximate position of the main resonances. The spectra show a striking landscape of transitions which show maxima or minima where $\frac{df}{dB} = 0$ and double-valued EPR resonant fields (i.e., transitions with EPR resonances at two different magnetic fields). No Boltzmann factor has been included in the simulation. The nuclear field splittings are unresolved and extremely small; they do not affect line intensities significantly.

The well-studied 4-state $S = 1/2$, $I = 1/2$ Si:P system can be mapped onto a two-qubit basis. With a 20-eigenstate state space, the Si:Bi spectrum is more complex, but we can identify a natural subset of 4 states (states 9,10,11,12), which represents an effective 2-coupled-qubit analogue As hyperpolarization initializes the spins in state $|10\rangle$ and this state has both the electron and nuclear spins fully anti-aligned with the magnetic field, it can be identified with the $(0)_e(0)_n$ state. Just as in the Si:P basis, the other states are related to it by either one or two qubit flips: $|10\rangle \rightarrow (0)_e(0)_n$; $|9\rangle \rightarrow (0)_e(1)_n$ $|12\rangle \rightarrow (1)_e(1)_n$; $|11\rangle \rightarrow (1)_e(0)_n$.

A sufficient requirement to execute a universal set of gates is the ability to perform arbitrary single qubit manipulations and a control-NOT (CNOT) gate [11]. In the two-qubit system described here, arbitrary electronic qubit-only manipulations can be performed with radiation pulses exciting transitions between states $12 \rightarrow 9$ and $10 \rightarrow 11$, while single nuclear-qubit rotations correspond to $12 \rightarrow 11$ and $10 \rightarrow 9$. The CNOT gate (for example, using the nuclear spin as a control qubit) is even simpler as it requires only a π pulse connecting $12 \rightarrow 9$ [9].

The electronic flips are EPR allowed at all fields for both Bi and P donors and so can be performed in a time on the order of 10 ns [3]. The nuclear transitions, however, require a slower (of the order of microseconds) NMR pulse for Si:P. For Si:Bi, on the other hand, at the $m = -4$ resonance the nuclear and electronic transition strengths become exactly equal as may be verified by setting $\theta_{-5} = 0$ and $\theta_{-4} = \pi/2$ in Eqs. (7) and (8). Time-dependent calculations [9] show that the duration of a π pulse is also equalized.

The $\omega_0 = A, 2A, 3A, 4A$ resonances yield textbook level anticrossings as well as "Bell-like" eigenstates. We do not consider the option of a "sudden" transfer of the latter to the high-field regime; ramping magnetic fields (up or down) sufficiently fast to violate adiabaticity, though not impossible, would require some of the fastest magnetic field pulses ever produced (e.g., 10^8 T/s obtained in Ref. [12]). However, we show that adiabatic magnetic field sweeps achievable by ordinary laboratory magnetic pulses (1–10 T/ms) suffice to achieve new possibilities.

The frequency minima at 5–8 GHz fields at which $df/dB = 0$ are expected to lead to a reduction of decoherence, since sensitivity to magnetic fluctuations is minimized; a measurable reduction has been seen [4] by varying the ratio df/dB by 30%–50%. In Fig. 2, we see that several transitions have a minimum frequency. These minima (in effect of $R_m + R_{m-1}$) occur for

$$\cos\theta_m = -\cos\theta_{m-1}. \tag{9}$$

Thus, $\theta_m = \pi - \theta_{m-1}$; the consequence is that the minima lie exactly midway in angular coordinates between cancellation resonances. For example, for the $12 \rightarrow 9$ line ($|+, m = -3\rangle \rightarrow |-, m = -4\rangle$) the minimum is at $\omega_0 = \frac{25A}{7} = 3.57A$ so $B \simeq 0.188$ T. Here, the $m = -4$ doublet has passed its resonance point at 0.21 T (for which $\theta_{-4} = \pi/2$) by an angle $\phi = \arccos(21/15\sqrt{2})$ and the $m = -3$ resonance is at an equal angular distance before its resonance at $\simeq 0.16$ T: Thus, $\theta_{-4} = \pi/2 + \phi$ while

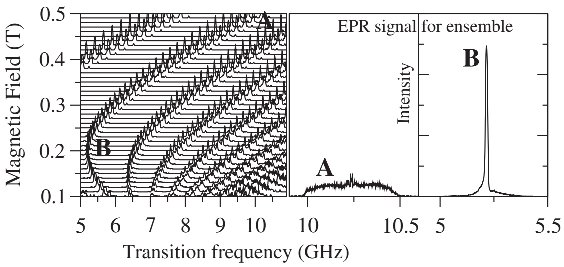

FIG. 3. The simulated EPR spectra for pairs of interacting Si:Bi donors shows ultranarrow lines at cancellation resonances, somewhat analogous to exact cancellation in ESEEM spectroscopy. The electronic spins are coupled by an exchange term $J\hat{\mathbf{S}}_1.\hat{\mathbf{S}}_2$. The left panel shows the effect of a typical $J = 0.5$ GHz coupling. A splitting (of order J) appears in general, but near the $\tilde{\omega}_0 = 4, 3$ resonances this is suppressed. The graphs on the right show the calculated signal from a sample of spins with a distribution of J, where average $\langle J \rangle = 0.3$ GHz, variance $\sigma_J = 0.3$. At the cancellation resonances, despite the ensemble averaging, the lines remain narrow.

$\theta_{-3} = \pi/2 - \phi$. Both doublets are quite close to the Bell-like form.

Line narrowing.—An interesting application arises for exchange coupling between Bi atoms. A pair of Bi atoms interacting via a spin-exchange term of the form $J\hat{\mathbf{S}}_1.\hat{\mathbf{S}}_2$ will result in splitting of the EPR spectral lines (with an energy splitting of order J). However, this is suppressed near the cancellation resonances. Analogously to exact cancellation, this makes the system less sensitive to ensemble averaging. For exact cancellation, this means the averaging over different orientations in powder spectra; here it means magnetic perturbations including spin-spin interactions. Figure 3 (left panel) plots the signal for $J = 0.5$ GHz for a single pair of Si:Bi atoms and clearly shows the line splitting away from the resonances. The right panels show the effects of averaging many spectra, each corresponding to different J (with an average $\langle J \rangle = 0.3$ GHz and width $\sigma_J = 0.3$ GHz). While typical spectra show a broad feature of width $\sim\sigma_J$, at the cancellation resonance the linewidth remains strikingly narrow (close to the single atom linewidth).

A frequency maximum at $\tilde{\omega}_0 = 7$ and $B \simeq 0.37$ T is marked with a 7 in Fig. 2(b). We can show that a $df/dB = 0$ point which is a maximum (in effect of $R_m - R_{m-1}$) implies

$$\cos\theta_m = \cos\theta_{m-1}. \qquad (10)$$

This condition does not correspond to the elimination of the field splitting terms; instead, it implies $\theta_{-3} = \theta_{-4} = \pi/4$, thus equalizing the Bloch angle for the associated energy levels. In this sense it is somewhat different from the other cancellation resonances; nevertheless, it still provides a $df/dB = 0$ point and thus some potential for reducing broadening and decoherence. In Ref. [9], it is shown that the $\tilde{\omega}_0 = 7$ resonance offers new possibilities for copying and storing qubit states. At $\tilde{\omega}_0 = 5$, the most drastic cancellation resonance occurs, since both σ_z and σ_x terms in Eq. (2) are eliminated, leaving only the isotropic term. Although there is no $df/dB = 0$ or line narrowing here, there is a possibility of driving, by a second-order process, simultaneous qubit rotations, e.g., $|0\rangle_e|1\rangle_n \to |1\rangle_e|0\rangle_n$; see [9].

Conclusions.—In the intermediate-field regime ($B \simeq 0.05$–0.6 T) the exceptionally large values of A and I for Si:Bi generate a series of cancellation resonances. They are associated not only with level crossing structures but also with more novel effects: Both line broadening and decoherence may be reduced; also, if the electronic and nuclear spins of Si:Bi are used as a 2-coupled qubit system, a universal set of quantum gates can be performed with fast EPR microwave pulses, eliminating the need for slower radio frequency addressing of the nuclear qubit. One scheme would envisage the following stages: (i) hyperpolarization of the sample into state $|10\rangle$ (in which the 2-qubit system is initialized as $|0\rangle_e|0\rangle_n$) at $B \approx 5$ T; (ii) a magnetic field pulse ($\sim$10 T/ms, of duration lower than decoherence times) would reduce B to $\simeq 0.1$ T; (iii) as the pulse ramps up, a large number of gates and operations on the system may be executed with fast EPR pulses; (iv) as the magnetic pulse decays, the system is restored to the (unmixed) high-B limit, leaving it in the desired superposition of $|0\rangle_e|0\rangle_n$, $|1\rangle_e|1\rangle_n$, $|0\rangle_e|1\rangle_n$, and $|1\rangle_e|0\rangle_n$ computational states. Thus, given the capability to rapidly ($\lesssim$1 ms) switch from the high- to intermediate-field regime, Si:Bi confers significant additional possibilities for quantum information processing relative to Si:P.

[1] B. E. Kane, Nature (London) **393**, 133 (1998).
[2] S. R. Schofield *et al.*, Phys. Rev. Lett. **91**, 136104 (2003); A. M. Tyryshkin *et al.*, Phys. Rev. B **68**, 193207 (2003); C. Fu Kai-Mei *et al.*, Phys. Rev. B **69**, 125306 (2004); G. W. Morley *et al.*, Phys. Rev. Lett. **101**, 207602 (2008); J. J. L. Morton *et al.* Nature (London) **455**, 1085 (2008); A. Morello *et al.*, Phys. Rev. B **80**, 081307(R) (2009).
[3] G. W. Morley *et al.*, arXiv:1004.3522 [Nature Mater. (to be published)].
[4] R. E. George *et al.*, preceding Letter, Phys. Rev. Lett. **105**, 067601 (2010).
[5] T. Sekiguchi *et al.*, Phys. Rev. Lett. **104**, 137402 (2010).
[6] H. Morishita *et al.*, Phys. Rev. B **80**, 205206 (2009).
[7] ENDOR is electron-nuclear double resonance; ESEEM is electron-spin echo envelope modulation.
[8] A. Schweiger and G. Jeschke, in *Principles of Pulse Paramagnetic Resonance* (Oxford University, New York, 2001).
[9] M. H. Mohammady, G. W. Morley, and T. S. Monteiro, arXiv:1006.3282.
[10] G. Mitrikas, Y. Sanakis, and G. Papavassiliou, Phys. Rev. A **81**, 020305(R) (2010).
[11] D. P. DiVincenzo, Phys. Rev. A **51**, 1015 (1995).
[12] J. Singleton, C. H. Mielke, A. Migliori, G. S. Boebinger, and A. H. Lacerda, Physica (Amsterdam) **346B**, 614 (2004).